Published in final edited form as:
FASEB J. 2007 June ; 21(8): 1788–1800.

Cannabinoid-2 receptor mediates protection against hepatic ischemia/reperfusion injury

Sándor Bátkai[*], **Douglas Osei-Hyiaman**[*], **Hao Pan**[*], **Osama El-Assal**[*], **Mohanraj Rajesh**[*], **Partha Mukhopadhyay**[*], **Feng Hong**[*], **Judith Harvey-White**[*], **Anjum Jafri**[*], **György Haskó**[†], **John W. Huffman**[‡], **Bin Gao**[*], **George Kunos**[*], and **Pál Pacher**[*,1]

[*] *Laboratory of Physiological Studies, National Institute on Alcohol Abuse and Alcoholism, National Institutes of Health, Bethesda, Maryland, USA*

† *Department of Surgery, University of Medicine and Dentistry of New Jersey-New Jersey Medical School, Newark, New Jersey, USA*

‡ *Howard L. Hunter Chemistry Laboratory, Clemson University, Clemson, South Carolina, USA*

Abstract

Hepatic ischemia-reperfusion (I/R) injury continues to be a fatal complication that can follow liver surgery or transplantation. We have investigated the involvement of the endocannabinoid system in hepatic I/R injury using an *in vivo* mouse model. Here we report that I/R triggers several-fold increases in the hepatic levels of the endocannabinoids anandamide and 2-arachidonoylglycerol, which originate from hepatocytes, Kupffer, and endothelial cells. The I/R-induced increased tissue endocannabinoid levels positively correlate with the degree of hepatic damage and serum TNF-α, MIP-1α, and MIP-2 levels. Furthermore, a brief exposure of hepatocytes to various oxidants (H_2O_2 and peroxynitrite) or inflammatory stimuli (endotoxin and TNF-α) also increases endocannabinoid levels. Activation of CB_2 cannabinoid receptors by JWH133 protects against I/R damage by decreasing inflammatory cell infiltration, tissue and serum TNF-α, MIP-1α and MIP-2 levels, tissue lipid peroxidation, and expression of adhesion molecule ICAM-1 *in vivo*. JWH133 also attenuates the TNF-α-induced ICAM-1 and VCAM-1 expression in human liver sinusoidal endothelial cells (HLSECs) and the adhesion of human neutrophils to HLSECs *in vitro*. Consistent with the protective role of CB_2 receptor activation, $CB_2^{-/-}$ mice develop increased I/R-induced tissue damage and proinflammatory phenotype. These findings suggest that oxidative/nitrosative stress and inflammatory stimuli may trigger endocannabinoid production, and indicate that targeting CB_2 cannabinoid receptors may represent a novel protective strategy against I/R injury. We also demonstrate that $CB_2^{-/-}$ mice have a normal hemodynamic profile.

Keywords

endocannabinoids; anandamide; 2-arachidonoylglycerol; peroxynitrite; oxidative stress

The endocannabinoid system is emerging as a promising new therapeutic target in inflammation, cancer, and metabolic, cardiovascular, gastrointestinal, and liver disorders [reviewed in (1–8)]. To date, two cannabinoid (CB) receptors have been identified by molecular cloning: the CB_1 receptor, which is highly expressed in the brain (9) but is also present in peripheral tissues, including the heart (10,11), vascular tissues (12,13), and liver (14–17), and the CB_2 receptor, expressed primarily by immune and hematopoietic cells [(18); reviewed in

[1] Correspondence: Section on Oxidative Stress and Tissue Injury, Laboratory of Physiologic Studies, National Institutes of Health/NIAAA, 5625 Fishers Lane, MSC-9413, Bethesda, Maryland 20892-9413, USA. E-mail: pacher@mail.nih.gov.

(7)]. The natural ligands of these receptors are lipid-like substances called endocannabinoids, which include arachidonoyl ethanolamide or anandamide (AEA), 2-arachidonoylglycerol (2-AG), and oleylethanolamide (OEA, reviewed in (7).

Cannabinoid CB_2 receptor knockout ($CB_2^{-/-}$) mice are fertile and care for their offspring and have similar phenotype as their wild-type littermates (19–22). Fluorescence-activated cell sorting analysis showed no differences in immune cell populations between $CB_2^{-/-}$ and $CB_2^{+/+}$ mice, while the immunomodulatory effects of delta (9) tetrahydrocannabinol were absent in knockouts (19–21). $CB_2^{-/-}$mice had elevated serum TNF-α levels compared with their wild-type littermates following a challenge with a low dose of endotoxin (22) and were characterized by markedly accelerated age-related trabecular bone loss and cortical expansion, although cortical thickness remains unaltered (23).

Organ injury, caused by transient ischemia followed by reperfusion (I/R), may develop in common diseases such as myocardial infarction and stroke, and may also accompany coronary bypass surgery and organ transplantation. The destructive effects of I/R arise from the acute generation of reactive oxygen species subsequent to reoxygenation, which inflict direct tissue damage and initiate a chain of deleterious cellular responses leading to inflammation, cell death, and eventually organ failure [reviewed in (24–29)].

Information about the role of cannabinoid receptor activation in cell protective mechanisms against I/R damage in the heart and brain remains limited and conflicting [reviewed in (7,30, 31)]. Most published studies were performed by using *ex vivo* models (*e.g.*, isolated perfused hearts), where the role of very important immunomodulatory effects of cannabinoids could not be evaluated, and/or used non-specific ligands for CB_2 receptors such as anandamide (2.3–32.3× less selective to CB_2 than to CB_1), WIN55212–2 (0.6–34× more selective to CB_2 than to CB_1), HU210 (1.7–8.6× less selective to CB_2 than to CB_1) with or without the CB_2 receptor selective antagonist/inverse agonist SR144528 to delineate the role of CB_2 receptors [reviewed in (7,32)].

Activation of CB_2 receptor by JWH133, which has been reported to be approx. 200× more selective to CB_2 than to CB_1 receptors (33), attenuated the inflammatory pain in rats (34,35) and experimental colitis in mice (36). In the present study we have used pharmacological agonist JWH-133, and antagonist/inverse agonist of cannabinoid CB_2 receptors SR144528, as well as CB_2 receptor knockout ($CB_2^{-/-}$) mice to study the role of the endocannabinoid system in an *in vivo* model of liver ischemia reperfusion. In addition, we studied the effects of JWH133 on TNF-α-induced ICAM-1 and VCAM-1 expression in human liver sinusoidal endothelial cells (HLSECs) and adhesion of human neutrophils to HLSECs *in vitro*. Furthermore, we have characterized the detailed hemodynamic profile of $CB_2^{-/-}$mice. Our results may also have relevance to the reperfusion injury of other organ systems, since I/R injury share similar pathophysiological mechanisms in many organs.

MATERIALS AND METHODS

Animals

All animal experiments conformed to NIH guidelines and were approved by the Institutional Animal Care and Use Committee of the National Institute on Alcohol Abuse and Alcoholism. $CB_2^{-/-}$ mice and their wild-type littermates were developed as described previously and had been backcrossed to a C57Bl/6J background (10,19,21–23). C57Bl/6J mice were obtained from The Jackson Laboratory (Bar Harbor, ME, USA).

Hepatic I/R protocol

Mice were anesthetized with pentobarbital (65 mg/kg i.p.). A midline laparotomy incision was performed to expose the liver. The hepatic artery and the portal vein were clamped using microaneurysm clamps. This model results in a segmental (70%) hepatic ischemia. This method of partial ischemia prevents mesenteric venous congestion by allowing portal decompression throughout the right and caudate lobes of the liver. The liver was kept moist at 37°C with gauze soaked in 0.9% saline. Body temperature was maintained at 37°C using a thermoregulatory heating blanket and by monitoring body temperature with a rectal temperature probe. Sham surgeries were identical except that hepatic blood flow was not reduced with a microaneurysm clamp. The duration of hepatic ischemia was 60 min in all experiments, after which the microaneurysm clamps were removed. The duration of the reperfusion was 90 min or 24 h, as indicated. After reperfusion, blood was collected and liver samples were removed, weighed, and snap-frozen in liquid nitrogen for determining biochemical parameters or fixed in 4% buffered formalin for histopathological evaluation.

Drugs

SR144528 (SR2) and SR141716 (SR1) were from the National Institute on Drug Abuse Drug Supply Program (Research Triangle Park, NC, USA). JWH133 was synthesized as described (33,37). AM251 and AM630 were from Tocris (Baldwin, MO, USA). All drugs were emulsified in corn oil–water (1:4) as described (10,11). All drugs were injected intraperitoneally 60 min prior to the occlusion of the hepatic artery and the portal vein. For cell culture experiments all lipid soluble drugs were dissolved in DMSO. All chemicals were from Sigma (St. Louis, MO, USA) except where mentioned otherwise.

Plasma AST and ALT levels

The activities of aspartate aminotransferase (AST) and alanine aminotransferase (ALT), indicators of liver damage, were measured in plasma samples using a clinical chemistry analyzer system (PROCHEM-V; Drew Scientific, Oxford, CT, USA).

Myeloperoxidase (MPO) activity

Myeloperoxidase activity was measured as described previously (38). Briefly, liver samples were homogenized (50 mg/ml) in 0.5% hexadecyltrimethylammonium bromide in 10 mM 3-(N-morpholino) propanesulfonic acid (MOPS) and centrifuged to separate the supernatant. An aliquot of the supernatant was mixed with a solution of 1.6 mM tetramethylbenzidine and 1 mM hydrogen peroxide. Activity was measured spectrophotometrically as the change in absorbance at 650 nm at 37°C, using a Spectramax microplate reader (Molecular Devices, Sunnyvale, CA, USA). MPO activity was expressed as mU/mg protein. Protein content was determined with the DC Protein assay (Bio-Rad, Hercules, CA, USA).

Lipid peroxidation

Malondialdehyde (MDA) formation was utilized to quantify the lipid peroxidation in tissues and measured as thiobarbituric acid-reactive material as described (38). Briefly, tissues were homogenized (100 mg/ml) in 1.15% KCl buffer. Homogenates (200 μl) were then added to a reaction mixture consisting of 1.5 ml of 0.8% thiobarbituric acid, 200 μl of 8.1% sodium dodecyl sulfate, 1.5 ml of 20% acetic acid (pH 3.5), and 600 μl of distilled H_2O and heated at 90°C for 45 min. After cooling to room temperature, the samples were cleared by centrifugation (10,000 *g*, 10 min), and their absorbance at A_{532} was measured with 1,1,3,3-tetramethoxypropane as an external standard. The level of lipid peroxides was expressed as nmol MDA/mg protein.

Levels and expression of TNF-α, MIP-1α, MIP-2, and ICAM-1

The levels of the inflammatory cytokine TNF-α and the chemokines MIP-1α and MIP-2 in plasma or homogenized liver tissue were determined using commercially available enzyme-linked immunosorbent assays (ELISA, R&D Systems, Minneapolis, MN, USA), according to the manufacturer's protocol as described previously (38). Expression of TNF-α, MIP-1α, MIP-2, and ICAM-1 in liver tissues was also determined from homogenized liver tissues employing RT-PCR.

Cell culture

Human liver sinusoidal endothelial cells (HLSECs) were obtained from Cell-Systems (Kirkland, WA, USA) and grown in CSC-complete growth medium according to the manufacturer's recommendations. Cells were grown in 0.2% gelatin-coated 100 mm cell culture dishes and used within 3–6 passages. Polymorphonuclear neutrophil leukocytes (PMN) were isolated from whole blood obtained from a healthy volunteer (NIH Clinical Center, Bethesda, MD, USA) using Ficoll hypaque (GE Biosciences, Piscataway, NJ, USA) density gradient solution. Primary mouse hepatocytes were isolated and cultured in Dulbecco's modified Eagle's medium (DMEM) containing 10% fetal bovine serum (FBS) and 100 U/ml penicillin and 100 μg/ml streptomycin.

Cell surface ICAM-1 and VCAM-1 expression

Cell surface expression of ICAM-1 and VCAM-1 were measured by *in situ* ELISA as described with modifications (39). In brief, HLSECs were grown in 96-well plates coated with 0.2% gelatin. The cells were treated with either TNF-α (50 ng/ml) ± JWH133 (0–4 μM) for 4 h. In some experiments, the cells were pretreated with either JWH133 (3 μM), SR1 or SR2, or AM 630, each used at the concentration of 1 μM for 1 h followed by incubation with TNF-α for 4 h. Then, cells were washed with phosphate buffered saline (PBS) and fixed in 4% formaldehyde (pH 7.4) and blocked with PBS containing 1% bovine serum albumin containing 100 mM glycine for 2 h at 4°C. The fixed monolayer was probed with either anti-human ICAM-1 or VCAM-1 monoclonal antibodies (R&D Systems, Minneapolis, MN, USA) for 1 h at 37°C and incubated with peroxidase-coupled anti-mouse (1:5000) (Pierce, Rockford, IL, USA) for 1 h at 37°C. Following washing, cells were incubated with 100 μl developing substrate solution (3, 3′, 5, 5′-tetramethyl-benzidine, Sigma) for 10 min and the reaction was terminated with 50 μl of 2N H_2SO_4, and the absorbance was measured at 450 nm. Each treatment was performed in triplicate and the experiments were repeated three times.

Polymorphonuclear neutrophil leukocytes (PMN)–endothelial cell adhesion

Neutrophil adhesion to endothelial cells was performed as described with modifications in the protocol (40). In brief, HLSECs were grown to confluence in 24-well plates and treated with TNF-α ± JWH133 or pretreated with CB_1/CB_2 antagonists followed by treatment with TNF-α/JWH133 as described above. Then, PMN were labeled with 2.5 μM Calcein-AM (Molecular Probes–Invitrogen, Carlsbad, CA, USA) for 1 h at 37°C in RPMI 1640 containing 1% FBS. HLSECs were washed twice with HLSECs basal medium and covered with 400 μl of HLSECs basal medium. Then 5×10^4/100 μl labeled PMN cells were added to HLSECs and incubated for 1 h at 37°C. After incubation, the monolayer was carefully washed with PBS to remove the unbound PMN. The adherent PMN were documented by Olympus IX 81 fluorescent microscope using 20× objective (Opelco, Dulles, VA, USA). Three fields were captured/experimental condition. Individual treatments were preformed in duplicate, and the entire set of experiments was repeated twice. The number of adherent PMN cells were counted using NIH Image J software and the values were expressed as PMN adhered/field.

Endocannabinoids

For measuring endocannabinoid levels, mice were euthanized and their livers were removed and extracted. Anandamide, 2-AG, and OEA levels were determined by liquid chromatography/mass spectrometry from liver tissues, isolated hepatocytes, and other cell fractions as described previously (10,41). Values are expressed as fmol or pmol/mg wet tissue or mg cell protein. In a separate set of experiments isolated primary hepatocytes were treated with TNF-α (100 ng/ml), endotoxin [1 μg/ml; lipopolysaccharide (LPS) from *Escherichia coli*, 0127:B8], H_2O_2 (100 μM) and peroxynitrite (50 μM) for 90 min, collected and processed in 5 ml PBS containing 200 μM PMSF, and processed for endocannabinoid measurements.

Histological analysis of liver samples

Liver samples were fixed in 4% buffered formalin. After embedding and cutting 5 μm slices, all sections were stained with hematoxylin/eosin (HE). Myeloperoxidase staining of neutrophils was done by using antimyeloperoxidase antibody according to the manufacturer's protocol (Zymed Lab., San Francisco, CA, USA), and samples were contrastained with nuclear fast red. Histological evaluation was performed in a blinded manner.

Hemodynamic measurements

Detailed hemodynamic measurements were conducted in mice anesthetized with 2% isoflurane by using Millar's pressure-volume system (Millar Instruments, Huston, TX, USA) as described previously (11,42).

Statistical analysis

Results are presented as means ± SEM. One-way ANOVA followed by Newman-Keuls multiple comparisons post-hoc analysis or unpaired *t* test for pair-wise comparisons and correlation between the variables (Pearson coefficient test) were calculated using the Graph Pad Prism 4 package (San Diego, CA, USA). $P < 0.05$ was considered significant.

RESULTS

Role of the CB_2 receptor in liver damage

Serum transaminase levels—For assessment of hepatocellular damage of the post-ischemic liver, the serum transaminase AST/ALT activities were measured. After 60 min of ischemia and subsequent 90-min reperfusion (60/90 min I/R), a dramatic increase in liver enzyme activities were observed in vehicle-treated C57Bl6/J mice as compared with sham-operated controls (Fig. 1). Pretreatment with 20 mg/kg of CB_2 agonist JWH133 significantly reduced the transaminase levels following I/R, and this effect was not prevented by the CB_1 selective antagonists AM251 (not shown), but was largely attenuated by the CB_2 selective antagonist SR144528. SR144528 alone showed a tendency to aggravate I/R damage, which did not reach statistical significance (not shown). In agreement with a protective role of CB_2 receptors suggested by the pharmacological findings, the liver damage to I/R was significantly more severe in CB_2 receptor knockout mice ($CB_2^{-/-}$) compared with wild-type littermates ($CB_2^{+/+}$) (Fig. 1*A*, *B*: right panels). The protective effect of JWH133 against I/R-induced liver damage was abolished in $CB_2^{-/-}$ mice (AST: 6440.63611.5 *vs*. 5900.03526.0 and ALT: 8735.4 ±716.6 *vs*. 8543.8±779.5; in $CB_2^{-/-}$ +vehicle *vs.* $CB_2^{-/-}$ +JWH133, respectively; $n=4$ in each group) subjected to 60/90 min I/R.

Neutrophil infiltration—An important factor in the tissue damage following I/R is neutrophil infiltration, an indicator of which is tissue MPO activity. In sham-operated wild-type mice MPO activity was barely detectable (Fig. 2*A*). 60/90 min I/R induced a marked increase in MPO activity, which was attenuated by JWH133. SR144528 pretreatment

prevented the effect of JWH133. Accordingly, the I/R-induced increase of MPO activity was significantly greater in $CB_2^{-/-}$ than in $CB_2^{+/+}$ mice (Fig. 2*A*), which is consistent with the more severe tissue damage observed in the former (Fig. 1*A*, *B*: right panels).

Lipid peroxidation—The rate of lipid peroxidation was negligible in sham-operated mice as indicated by the low MDA content. MDA content nearly doubled following 60/90 min I/R and this increase was attenuated in mice pretreated with JWH133, an effect preventable by SR144528 pre-treatment (Fig. 2*B*: left panel). Again, I/R caused a greater increase in MDA in $CB_2^{-/-}$ than in $CB_2^{+/+}$ mice (Fig. 2*B*: right panel).

Proinflammatory cytokine and chemokine expression in liver and serum—60/90 min I/R greatly increased the expression of TNF-α, MIP-1α, MIP-2, and ICAM-1 in liver tissue, as documented by RT-PCR (Fig. 3*A*), with concomitant increase of their levels in both liver homogenates and in the serum, as detected by ELISA (Fig. 3*B*, *C*). JWH133 significantly attenuated the I/R-induced increase in cytokine levels in both liver and serum, whereas SR144528 pretreatment largely prevented these effects of JWH133 (Fig. 3*B*, *C*). Inflammatory markers were significantly more elevated following 60/90 min I/R in $CB_2^{-/-}$ as compared to $CB_2^{+/+}$ mice (Fig. 3*A*–*C*).

Hepatic histopathology following I/R—Sham-operated mice showed normal hepatic histology (Fig. 4*A*). In mice 24 h following ischemic injury (60 min I), there was a marked degree of reperfusion damage indicated by the necrosis of hepatocytes in the pericentral and midzonal regions, and by the massive neutrophil infiltration in the damaged areas (Fig. 4*A*, *B*). The tissue injury and neutrophil infiltration were less pronounced in the JWH133-treated group and more extensive in the $CB_2^{-/-}$ mice (Fig. 4*A*, *B*).

JWH133 mitigates TNF-α induced ICAM-1 and VCAM-1 expression—TNF-α (50 ng/ml) treatment of HLSECs for 4 h resulted in robust activation of ICAM-1 (~5 fold, Fig. 5*A*) and VCAM-1 (~4-fold, Fig. 5*C*), respectively, when compared with control. JWH133 (0.5–4 μM) dose dependently inhibited the TNF-α induced increased expression levels of both ICAM-1 and VCAM-1 (Fig. 5*A*, *C*), which was attenuated by CB_2 antagonists (SR 2 or AM 630; 1 μM), but not CB_1 antagonists (SR1; 1 μM, not shown) (Fig. 5*B*, *D*). Antagonists had no effect in controls or TNF-α treated cells.

JWH133 inhibits TNF-α induced PMN adhesion to HLSECs—TNF-α (50 ng/ml) treatment, resulted in enhanced PMN adhesion to HLSECs (~3.5-fold) compared with control (Fig. 5*E*). JWH133 (3 μM) pretreatment markedly inhibited TNF-α induced PMN adhesion to HLSECs and this effect was prevented by CB_2 antagonists. Antagonists had no effect in controls or TNF-α treated cells on PMN adhesion.

I/R increases endocannabinoid levels in liver tissue and in various liver cell fractions—Ischemia/reperfusion (60/90 min) but not ischemia (60 min) alone led to substantial increases in liver tissue content of the endocannabinoids anandamide (AEA) and 2-arachidonoylglycerol (2-AG) as well as the related lipid oleoylethanolamide (OEA, Fig. 6*A*). Similarly, the levels of these lipids were increased in the purified hepatocyte fraction (Fig. 6*B*) as well as in the Kupffer cell/endothelial cell fraction of isolated liver cells (except for 2-AG in the latter; Fig. 6*C*).

Tissue endocannabinoid levels positively correlate with markers of tissue damage and inflammation—Significant correlation was found between hepatic AEA and 2-AG and the plasma transaminase levels: AEA *vs*. ALT and AEA *vs*. AST, r: 0.77 and r: 0.73, ($P<0.0001$; respectively, Fig. 7) following 60/90 min I/R. Similarly, chemokine-cytokine

levels and hepatic AEA and 2-AG content correlated significantly. TNF-α levels correlated with the hepatic content of all three lipids (AEA r: 0.52, *P*=0.008; 2-AG r: 0.73, *P*=0.0004; OEA r: 0.7, *P*=0.0095), whereas MIP-1α and MIP-2 levels correlated only with AEA (r: 0.42, *P*=0.024 and r: 0.5, *P*=0.01, respectively, Fig. 7).

Inflammatory stimuli (TNF-α and endotoxin) and oxidants (H_2O_2 and peroxynitrite) increase endocannabinoid levels in hepatocytes *in vitro*—TNF-α, endotoxin (LPS), H_2O_2, and peroxynitrite ($ONOO^-$) exposure of isolated primary hepatocytes for 90 min markedly increased endocannabinoid levels in these cells (especially AEA and OEA; Fig. 8).

Hemodynamics—JWH133 had no effect on hemodynamic variables of control mice (20 mg/kg i.p. injection, Table 1). Furthermore, $CB_2^{-/-}$ mice had normal hemodynamic profile, the parameters in Table 2 are not significantly different from their wild-type littermates.

DISCUSSION

The hypothesis on the role of the endocannabinoid system in I/R is controversial, as it has been derived from a few studies using isolated organs and is based on results obtained mostly through the use of pharmacological agents (7,30,31). In the present study, we used agonists and antagonists of the cannabinoid CB_2 receptor as well as CB_2 receptor knockout mice to delineate the role of the endocannabinoid system in an *in vivo* model of liver ischemia reperfusion (I/R).

We demonstrate that pretreatment of mice with a CB_2 receptor agonist JWH133 decreases inflammatory cell infiltration, tissue and serum TNF-α, MIP-1α and MIP-2 levels, tissue lipid peroxidation, and tissue expression of adhesion molecule ICAM-1. CB_2 activation also attenuates the TNF-α-induced ICAM-1 and VCAM-1 expression in human liver sinusoidal endothelial cells (HLSECs) and adhesion of human neutrophils to HLSECs *in vitro*.

Importantly, these findings suggest that targeting CB_2 cannabinoid receptors may represent a novel strategy in protecting against hepatic I/R injury. In contrast, $CB_2^{-/-}$ mice develop increased I/R-induced tissue damage and proinflammatory phenotype. I/R, but not ischemia alone, triggers several-fold increases in the hepatic levels of the endocannabinoids anandamide and 2-AG, which originate from hepatocytes, Kupffer, and endothelial cells. These increases positively correlate with the degree of tissue damage and serum TNF-α, MIP-1α, and MIP-2 levels. Consistently, brief exposure of primary hepatocytes to various oxidants, (H_2O_2, peroxynitrite) or inflammatory stimuli (TNF-α endotoxin), which are important mediators of reperfusion damage (24–29,43), triggers marked increase in cellular endocannabinoid levels. Thus, not only inflammatory stimuli (*e.g.*, endotoxin and TNF-α), but also oxidative/nitrosative stress, can modulate endocannabinoid levels in hepatocytes, and most likely in most other cell types, too. Therefore, parenchymal cells may also represent a very significant source of endocannabinoids produced in various pathological conditions associated with increased inflammation and oxidative tissue injury, in addition to the previously reported activated macrophages (reviewed in 7). Our findings also suggest that an I/R-induced activation of hepatic endocannabinoids may limit the extent of tissue injury via stimlation of CB_2 receptors.

Increased brain endocannabinoid levels during ischemic brain injury were reported by several studies (44–47). However, the role of endocannabinoids and CB_1 receptor activation in cerebral I/R remains controversial. Anandamide, 2-AG, as well as the synthetic cannabinoid WIN 55,212–2, were found to protect cultured cortical neurons against hypoxia and glucose deprivation by a mechanism not involving $CB_{1/2}$ receptors (48,49). In contrast, *in vivo* treatment with WIN 55,212–2 or the CB_1 agonist BAY38–7271 reduced infarct size following cerebral ischemia in rats via activation of CB_1 receptors (48,50). Consistent with the CB_1-

mediated cerebro-protection, infarct size and mortality following cerebral ischemic injury were greater in CB_1 knockout mice than in their wild-type littermates (51). The protective role of CB_1 receptor stimulation against cerebral ischemia was confirmed by a more recent study using the synthetic cannabinoid HU-210, the protective effect of which could be attributed to CB_1-mediated hypothermia (52). Likewise, CB_1-mediated hypothermia was responsible for the neuroprotective effects of delta (9)-tetrahydrocannabinol in a mouse ischemic model of cerebral injury (53), and perhaps also in a rat model of global cerebral ischemia (54). In contrast, other studies do not support the neuroprotective role of endocannabinoids and CB_1 receptor activation. In fact, the CB_1 antagonists SR141716 and LY320135 were found to reduce infarct size and to improve neurological function in a rat model of cerebral ischemia (46,47).

Endocannabinoids acting via CB_1/CB_2-dependent, or CB_1/CB_2-independent mechanisms have also been implicated in the protection conferred by various forms of preconditioning (including ischemic) of the myocardium [reviewed in (7,30,55)]. However, a major limitation of these studies is the use of buffer-perfused isolated heart preparations, in which the effects of endocannabinoids and synthetic agonists on immune cells, which are pivotal in reperfusion damage, cannot be studied, as well as the use of nonselective cannabinoid ligands (7,30). In a more relevant whole animal model of myocardial I/R injury induced by coronary occlusion/reocclusion in anesthetized mice, the published evidence points to the protective role CB_2 but not CB_1 receptor activation [reviewed in (7,55)]. In a recent study using nonselective CB agonist WIN55212–2 and CB_2 antagonist AM630 in a mouse model of myocardial I/R, the reduction of leukocyte-dependent myocardial damage could be attributed to CB_2 receptor activation since the protection afforded by WIN55212–2 could be prevented by AM630, but not by CB_1 antagonist AM251 (56). In agreement with those findings, pretreatment of mice in the present study with the selective CB_2 agonist JWH133 afforded protection against hepatic I/R damage by decreasing inflammatory cell infiltration and consequent inflammatory damage. This protective effect as well as the decreased inflammatory cell infiltration were attenuated by a selective CB_2 receptor antagonist and in CB_2 knockout mice, further confirming the role of CB_2 receptors in these events. Consistently, CB_2 receptor knockout mice developed increased injury and proinflammatory phenotype following I/R.

It is well established that liver I/R injury is dependent on PMN infiltration, Kupffer cell activation, and cytokine response (57–60). Adhesion molecules mediate the initial attachment of neutrophils to the activated endothelium (58,61). On reperfusion, TNF-α acts as a continuous stimulator for neutrophil infiltration in the liver and it also up-regulates the production of cell-type specific leukocyte chemoattractants, known as chemokines, which have also been shown to cause up-regulation of cell adhesion molecules and neutrophil activation (59). The increased inflammatory response further aggravates oxidative stress and initiates a chain of deleterious events eventually culminating in cellular dysfunction and death. As demonstrated by the present findings and illustrated in the proposed schematic diagram (Fig. 9), CB_2 receptor stimulation limits hepatic injury by decreasing the expression of ICAM-1, VCAM-1, neutrophil infiltration, TNF-α, chemokine (MIP-1α and MIP-2) levels, and lipid peroxidation. The decrease in lipid peroxidation can be secondary to the decrease of inflammatory cell infiltration and activation.

Hepatic ischemia/reperfusion or exposure of primary hepatocytes to various inflammatory stimuli or oxidants triggered marked increases in the cellular endocannabinoid levels, which were positively correlated with the degree of tissue damage and inflammatory markers. Our findings suggest that these endocannabinoids may limit hepatic injury by modulating the expression of adhesion molecules and the infiltration and activation of inflammatory cells by CB_2-dependent mechanisms, which is also consistent with the emerging role of CB_2 receptors in regulating microglial cell function and neuroinflammation (62,63). Both mononuclear and polymorphonuclear leukocytes are known to express CB_2 receptors (29,64), which could be

activated on these infiltrating cells through a paracrine mechanism by endocannabinoids generated in and released from the various cell types in the liver.

It is noteworthy that the endocannabinoid anandamide can promote stellate cell and hepatocyte apoptosis *in vitro* by a mechanism not related to CB receptors (65,66). Thus, the role of endocannabinoids in liver injury is still a very controversial issue requiring further clarification [reviewed in (3,4,6,7)].

Collectively, our results suggest that treatment with selective CB_2 cannabinoid agonists may be useful in protecting the liver as well as other tissues against I/R injury. This is particularly encouraging since CB_2 receptor stimulation is not associated with psychoactive effects and was also found to mediate antifibrogenic effects in the liver (67). Even though the protection afforded by JWH133 in hepatic I/R was lost in CB_2 knockout mice and attenuated by CB_2 antagonist, which clearly indicates CB_2 receptor involvement, as with any drugs available, it cannot be excluded that JWH133 has some additional beneficial effects not related to CB_2 receptor activation.

Acknowledgements

This study was supported by the Intramural Research Program of NIH/NIAAA (to P.P.) and NIDA grant DA03590 (to J.W.H.).

References

1. Di Marzo V, Bifulco M, De Petrocellis L. The endocannabinoid system and its therapeutic exploitation. Nat Rev Drug Discov 2004;3:771–784. [PubMed: 15340387]
2. Massa F, Storr M, Lutz B. The endocannabinoid system in the physiology and pathophysiology of the gastrointestinal tract. J Mol Med 2005;83:944–954. [PubMed: 16133420]
3. Gabbay E, Avraham Y, Ilan Y, Israeli E, Berry EM. Endocannabinoids and liver disease–review. Liver Int 2005;25:921–926. [PubMed: 16162147]
4. Zamora-Valdes D, Ponciano-Rodriguez G, Chavez-Tapia NC, Mendez-Sanchez N. The endocannabinoid system in chronic liver disease. Ann Hepatol 2005;4:248–254. [PubMed: 16432489]
5. Pacher P, Batkai S, Kunos G. Cirrhotic cardiomyopathy: an endocannabinoid connection. Br J Pharmacol 2005;146:313–314. [PubMed: 16025137]
6. Mallat A, Lotersztajn S. Endocannabinoids as novel mediators of liver diseases. J Endocrinol Invest 2006;29:58–65. [PubMed: 16751709]
7. Pacher P, Batkai S, Kunos G. The endocannabinoid system as an emerging target of pharmacotherapy. Pharmacol Rev 2006;58:389–462. [PubMed: 16968947]
8. Kunos G, Osei-Hyiaman D, Batkai S, Gao B. Cannabinoids hurt, heal in cirrhosis. Nat Med 2006;12:608–610. [PubMed: 16761000]
9. Matsuda LA, Lolait SJ, Brownstein MJ, Young AC, Bonner TI. Structure of a cannabinoid receptor and functional expression of the cloned cDNA. Nature 1990;346:561–564. [PubMed: 2165569]
10. Batkai S, Pacher P, Osei-Hyiaman D, Radaeva S, Liu J, Harvey-White J, Offertaler L, Mackie K, Rudd MA, Bukoski RD, Kunos G. Endocannabinoids acting at cannabinoid-1 receptors regulate cardiovascular function in hypertension. Circulation 2004;110:1996–2002. [PubMed: 15451779]
11. Pacher P, Batkai S, Osei-Hyiaman D, Offertaler L, Liu J, Harvey-White J, Brassai A, Jarai Z, Cravatt BF, Kunos G. Hemodynamic profile, responsiveness to anandamide, and baroreflex sensitivity of mice lacking fatty acid amide hydrolase. Am J Physiol Heart Circ Physiol 2005;289:H533–541. [PubMed: 15821037]
12. Gebremedhin D, Lange AR, Campbell WB, Hillard CJ, Harder DR. Cannabinoid CB1 receptor of cat cerebral arterial muscle functions to inhibit L-type Ca2+ channel current. Amer J Physiol 1999;276:H2085–2093. [PubMed: 10362691]
13. Liu J, Gao B, Mirshahi F, Sanyal AJ, Khanolkar AD, Makriyannis A, Kunos G. Functional CB1 cannabinoid receptors in human vascular endothelial cells. Biochem J 346, Pt 2000;3:835–840. [PubMed: 10698714]

14. Batkai S, Jarai Z, Wagner JA, Goparaju SK, Varga K, Liu J, Wang L, Mirshahi F, Khanolkar AD, Makriyannis A, Urbaschek R, Garcia N Jr, Sanyal AJ, Kunos G. Endocannabinoids acting at vascular CB1 receptors mediate the vasodilated state in advanced liver cirrhosis. Nat Med 2001;7:827–832. [PubMed: 11433348]
15. Engeli S, Bohnke J, Feldpausch M, Gorzelniak K, Janke J, Batkai S, Pacher P, Harvey-White J, Luft FC, Sharma AM, Jordan J. Activation of the peripheral endocannabinoid system in human obesity. Diabetes 2005;54:2838–2843. [PubMed: 16186383]
16. Osei-Hyiaman D, DePetrillo M, Pacher P, Liu J, Radaeva S, Batkai S, Harvey-White J, Mackie K, Offertaler L, Wang L, Kunos G. Endocannabinoid activation at hepatic CB1 receptors stimulates fatty acid synthesis and contributes to diet-induced obesity. J Clin Invest 2005;115:1298–1305. [PubMed: 15864349]
17. Teixeira-Clerc F, Julien B, Grenard P, Tran Van Nhieu J, Deveaux V, Li L, Serriere-Lanneau V, Ledent C, Mallat A, Lotersztajn S. CB1 cannabinoid receptor antagonism: a new strategy for the treatment of liver fibrosis. Nat Med 2006;12:671–676. [PubMed: 16715087]
18. Munro S, Thomas KL, Abu-Shaar M. Molecular characterization of a peripheral receptor for cannabinoids. Nature 1993;365:61–65. [PubMed: 7689702]
19. Jarai Z, Wagner JA, Varga K, Lake KD, Compton DR, Martin BR, Zimmer AM, Bonner TI, Buckley NE, Mezey E, Razdan RK, Zimmer A, Kunos G. Cannabinoid-induced mesenteric vasodilation through an endothelial site distinct from CB1 or CB2 receptors. Proceed Nat Acad Sci USA 1999;96:14136–14141.
20. Buckley NE, McCoy KL, Mezey E, Bonner T, Zimmer A, Felder CC, Glass M, Zimmer A. Immunomodulation by cannabinoids is absent in mice deficient for the cannabinoid CB(2) receptor. Eur J Pharmacol 2000;396:141–149. [PubMed: 10822068]
21. Batkai S, Pacher P, Jarai Z, Wagner JA, Kunos G. Cannabinoid antagonist SR-141716 inhibits endotoxic hypotension by a cardiac mechanism not involving CB1 or CB2 receptors. Am J Physiol Heart Circ Physiol 2004;287:H595–600. [PubMed: 15059774]
22. Milman G, Maor Y, Abu-Lafi S, Horowitz M, Gallily R, Batkai S, Mo FM, Offertaler L, Pacher P, Kunos G, Mechoulam R. N-arachidonoyl L-serine, an endocannabinoid-like brain constituent with vasodilatory properties. Proc Nat Acad Sci USA 2006;103:2428–2433. [PubMed: 16467152]
23. Ofek O, Karsak M, Leclerc N, Fogel M, Frenkel B, Wright K, Tam J, Attar-Namdar M, Kram V, Shohami E, Mechoulam R, Zimmer A, Bab I. Peripheral cannabinoid receptor, CB2, regulates bone mass. Proc Nat Acad Sci USA 2006;103:696–701. [PubMed: 16407142]
24. Fan C, Zwacka RM, Engelhardt JF. Therapeutic approaches for ischemia/reperfusion injury in the liver. J Mol Med 1999;77:577–592. [PubMed: 10543390]
25. Jaeschke H, Lemasters JJ. Apoptosis versus oncotic necrosis in hepatic ischemia/reperfusion injury. Gastroenterology 2003;125:1246–1257. [PubMed: 14517806]
26. Kupiec-Weglinski JW, Busuttil RW. Ischemia and reperfusion injury in liver transplantation. Transpl Proc 2005;37:1653–1656.
27. Husted TL, Lentsch AB. Anti-inflammatory approaches to the prevention of ischemia/reperfusion injury in solid organ transplantation. Curr Opin Investig Drugs 2005;6:508–512.
28. Szabo G, Bahrle S. Role of nitrosative stress and poly(ADP-ribose) polymerase activation in myocardial reperfusion injury. Curr Vasc Pharmacol 2005;3:215–220. [PubMed: 16026318]
29. Pacher P, Nivorozhkin A, Szabo C. Therapeutic effects of xanthine oxidase inhibitors: renaissance half a century after the discovery of allopurinol. Pharmacol Rev 2006;58:87–114. [PubMed: 16507884]
30. Pacher, P.; Batkai, S.; Kunos, G. Handbook of Experimental Pharmacology. 2005. Cardiovascular pharmacology of cannabinoids; p. 599-625.
31. Pacher P, Batkai S, Kunos G. Blood pressure regulation by endocannabinoids and their receptors. Neuropharmacology 2005;48:1130–1138. [PubMed: 15910888]
32. Pertwee, RG. Handbook of Experimental Pharmacology. 2005. Pharmacological actions of cannabinoids; p. 1-51.
33. Huffman JW, Liddle J, Yu S, Aung MM, Abood ME, Wiley JL, Martin BR. 3-(1′,1′-Dimethylbutyl)-1-deoxy-delta8-THC and related compounds: synthesis of selective ligands for the CB2 receptor. Bioorg Med Chem 1999;7:2905–2914. [PubMed: 10658595]

34. Elmes SJ, Jhaveri MD, Smart D, Kendall DA, Chapman V. Cannabinoid CB2 receptor activation inhibits mechanically evoked responses of wide dynamic range dorsal horn neurons in naive rats and in rat models of inflammatory and neuropathic pain. Eur J Neurosci 2004;20:2311–2320. [PubMed: 15525273]
35. Elmes SJ, Winyard LA, Medhurst SJ, Clayton NM, Wilson AW, Kendall DA, Chapman V. Activation of CB1 and CB2 receptors attenuates the induction and maintenance of inflammatory pain in the rat. Pain 2005;118:327–335. [PubMed: 16289798]
36. Kimball ES, Schneider CR, Wallace NH, Hornby PJ. Agonists of cannabinoid receptor 1 and 2 inhibit experimental colitis induced by oil of mustard and by dextran sulfate sodium. Amer J Physiol 2006;291:G364–371.
37. Huffman JW. CB2 receptor ligands. Mini Rev Med Chem 2005;5:641–649. [PubMed: 16026310]
38. Liaudet L, Murthy KG, Mabley JG, Pacher P, Soriano FG, Salzman AL, Szabo C. Comparison of inflammation, organ damage, and oxidant stress induced by Salmonella enterica serovar Muenchen flagellin and serovar Enteritidis lipopolysaccharide. Infect Immun 2002;70:192–198. [PubMed: 11748182]
39. Bhunia AK, Arai T, Bulkley G, Chatterjee S. Lactosylceramide mediates tumor necrosis factor-alpha-induced intercellular adhesion molecule-1 (ICAM-1) expression and the adhesion of neutrophil in human umbilical vein endothelial cells. J Biol Chem 1998;273:34349–34357. [PubMed: 9852101]
40. Arai T, Bhunia AK, Chatterjee S, Bulkley GB. Lactosylceramide stimulates human neutrophils to upregulate Mac-1, adhere to endothelium, and generate reactive oxygen metabolites in vitro. Circ Res 1998;82:540–547. [PubMed: 9529158]
41. Wang L, Liu J, Harvey-White J, Zimmer A, Kunos G. Endocannabinoid signaling via cannabinoid receptor 1 is involved in ethanol preference and its age-dependent decline in mice. Proc Nat Acad Sci USA 2003;100:1393–1398. [PubMed: 12538878]
42. Pacher P, Batkai S, Kunos G. Haemodynamic profile and responsiveness to anandamide of TRPV1 receptor knock-out mice. J Physiol 2004;558:647–657. [PubMed: 15121805]
43. Pacher P, Beckman JS, Liaudet L. Nitric oxide and peroxynitrite in health and disease. Physiol Rev 2007;87:315–424. [PubMed: 17237348]
44. Schmid PC, Krebsbach RJ, Perry SR, Dettmer TM, Maasson JL, Schmid HH. Occurrence and postmortem generation of anandamide and other long-chain N-acylethanolamines in mammalian brain. FEBS Lett 1995;375:117–120. [PubMed: 7498458]
45. Schabitz WR, Giuffrida A, Berger C, Aschoff A, Schwaninger M, Schwab S, Piomelli D. Release of fatty acid amides in a patient with hemispheric stroke: a microdialysis study. Stroke 2002;33:2112–2114. [PubMed: 12154273]
46. Berger C, Schmid PC, Schabitz WR, Wolf M, Schwab S, Schmid HH. Massive accumulation of N-acylethanolamines after stroke. Cell signalling in acute cerebral ischemia. J Neurochem 2004;88:1159–1167. [PubMed: 15009671]
47. Muthian S, Rademacher DJ, Roelke CT, Gross GJ, Hillard CJ. Anandamide content is increased and CB1 cannabinoid receptor blockade is protective during transient, focal cerebral ischemia. Neuroscience 2004;129:743–750. [PubMed: 15541895]
48. Nagayama T, Sinor AD, Simon RP, Chen J, Graham SH, Jin K, Greenberg DA. Cannabinoids and neuroprotection in global and focal cerebral ischemia and in neuronal cultures. J Neurosci 1999;19:2987–2995. [PubMed: 10191316]
49. Sinor AD, Irvin SM, Greenberg DA. Endocannabinoids protect cerebral cortical neurons from in vitro ischemia in rats. Neurosci Lett 2000;278:157–160. [PubMed: 10653017]
50. Mauler F, Mittendorf J, Horvath E, De Vry J. Characterization of the diarylether sulfonylester (−)-(R)-3-(2-hydroxymethylindanyl-4-oxy)phenyl-4,4,4-trifluoro-1-sulfonate (BAY 38–7271) as a potent cannabinoid receptor agonist with neuroprotective properties. J Pharmacol Exp Ther 2002;302:359–368. [PubMed: 12065738]
51. Parmentier-Batteur S, Jin K, Mao XO, Xie L, Greenberg DA. Increased severity of stroke in CB1 cannabinoid receptor knock-out mice. J Neurosci 2002;22:9771–9775. [PubMed: 12427832]
52. Leker RR, Gai N, Mechoulam R, Ovadia H. Drug-induced hypothermia reduces ischemic damage: effects of the cannabinoid HU-210. Stroke 2003;34:2000–2006. [PubMed: 12829867]

53. Hayakawa K, Mishima K, Abe K, Hasebe N, Takamatsu F, Yasuda H, Ikeda T, Inui K, Egashira N, Iwasaki K, Fujiwara M. Cannabidiol prevents infarction via the non-CB1 cannabinoid receptor mechanism. Neuroreport 2004;15:2381–2385. [PubMed: 15640760]
54. Louw DF, Yang FW, Sutherland GR. The effect of delta-9-tetrahydrocannabinol on forebrain ischemia in rat. Brain Res 2000;857:183–187. [PubMed: 10700566]
55. Lamontagne D, Lepicier P, Lagneux C, Bouchard JF. The endogenous cardiac cannabinoid system: a new protective mechanism against myocardial ischemia. Arch Mal Coeur Vaiss 2006;99:242–246. [PubMed: 16618028]
56. Di Filippo C, Rossi F, Rossi S, D'Amico M. Cannabinoid CB2 receptor activation reduces mouse myocardial ischemia-reperfusion injury: involvement of cytokine/chemokines and PMN. J Leuk Biol 2004;75:453–459.
57. Jaeschke H, Smith CW, Clemens MG, Ganey PE, Roth RA. Mechanisms of inflammatory liver injury: adhesion molecules and cytotoxicity of neutrophils. Toxicol Appl Pharmacol 1996;139:213–226. [PubMed: 8806837]
58. Jaeschke H. Cellular adhesion molecules: regulation and functional significance in the pathogenesis of liver diseases. Amer J Physiol 1997;273:G602–611. [PubMed: 9341049]
59. Jaeschke H. Mechanisms of liver injury. II Mechanisms of neutrophil-induced liver cell injury during hepatic ischemia-reperfusion and other acute inflammatory conditions. Amer J Physiol 2006;290:G1083–1088.
60. Ohkohchi N, Shibuya H, Tsukamoto S, Sakurada M, Oikawa K, Terashima T, Satomi S. Kupffer's cells modulate neutrophile activity by superoxide anion and tumor necrosis factor-delta in reperfusion injury of liver transplantation-mechanisms of radical generation and reperfusion injury after cold ischemia. Transplantation Proc 1999;31:1055–1058.
61. Carlos TM, Harlan JM. Leukocyte-endothelial adhesion molecules. Blood 1994;84:2068–2101. [PubMed: 7522621]
62. Walter L, Stella N. Cannabinoids and neuroinflammation. Br J Pharmacol 2004;141:775–785. [PubMed: 14757702]
63. Maresz K, Carrier EJ, Ponomarev ED, Hillard CJ, Dittel BN. Modulation of the cannabinoid CB2 receptor in microglial cells in response to inflammatory stimuli. J Neurochem 2005;95:437–445. [PubMed: 16086683]
64. Klein TW. Cannabinoid-based drugs as anti-inflammatory therapeutics. Nat Rev Immunol 2005;5:400–411. [PubMed: 15864274]
65. Siegmund SV, Uchinami H, Osawa Y, Brenner DA, Schwabe RF. Anandamide induces necrosis in primary hepatic stellate cells. Hepatology 2005;41:1085–1095. [PubMed: 15841466]
66. Siegmund SV, Seki E, Osawa Y, Uchinami H, Cravatt BF, Schwabe RF. Fatty acid amide hydrolase determines anandamide-induced cell death in the liver. J Biol Chem 2006;281:10431–10438. [PubMed: 16418162]
67. Julien B, Grenard P, Teixeira-Clerc F, Van Nhieu JT, Li L, Karsak M, Zimmer A, Mallat A, Lotersztajn S. Antifibrogenic role of the cannabinoid receptor CB2 in the liver. Gastroenterology 2005;128:742–755. [PubMed: 15765409]

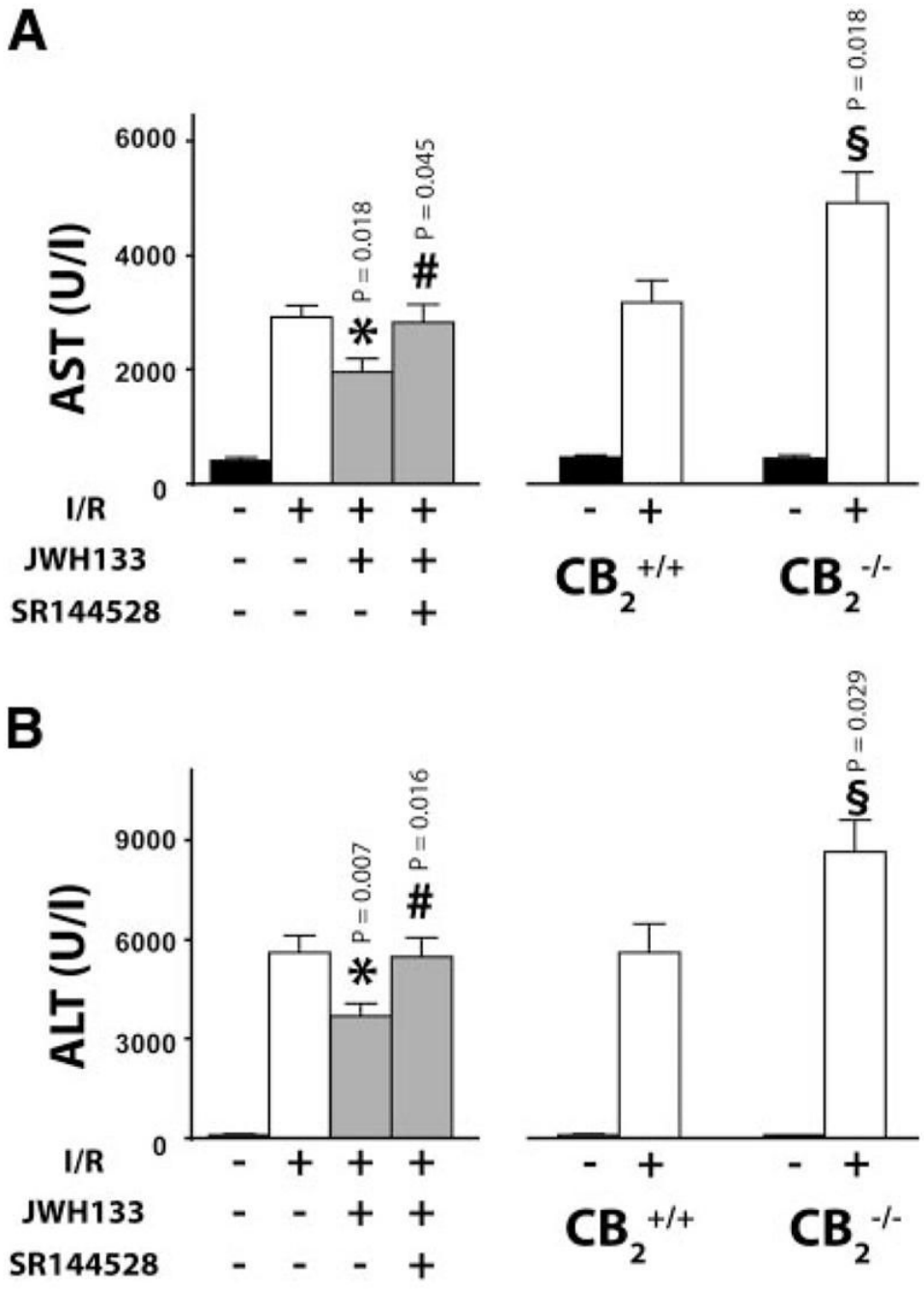

Figure 1.

Role of CB_2 receptor in liver I/R injury. Left: Serum transaminase AST (*A*) and ALT (*B*) levels in sham (*n*=14) or in mice exposed to 60/90 min I/R, pretreated with vehicle (*n*=14), JWH133 (20 mg/kg, *n*=20), or SR144528 (3 mg/kg) in combination with JWH133 (*n*=13). Right: Serum transaminase AST (*A*) and ALT (*B*) levels in sham $CB_2^{+/+}$ (*n*=7) and $CB_2^{-/-}$ mice (*n*=7) or in $CB_2^{+/+}$ (*n*=11) and $CB_2^{-/-}$ (*n*=17) mice exposed to I/R. (*P<0.05: I/R in vehicle- *vs*. JWH133-treated; #P<0.05: I/R in JWH133- *vs*. SR144528+JWH133-treated; §P<0.05: IR in $CB_2^{-/-}$*vs*. $CB_2^{+/+}$).

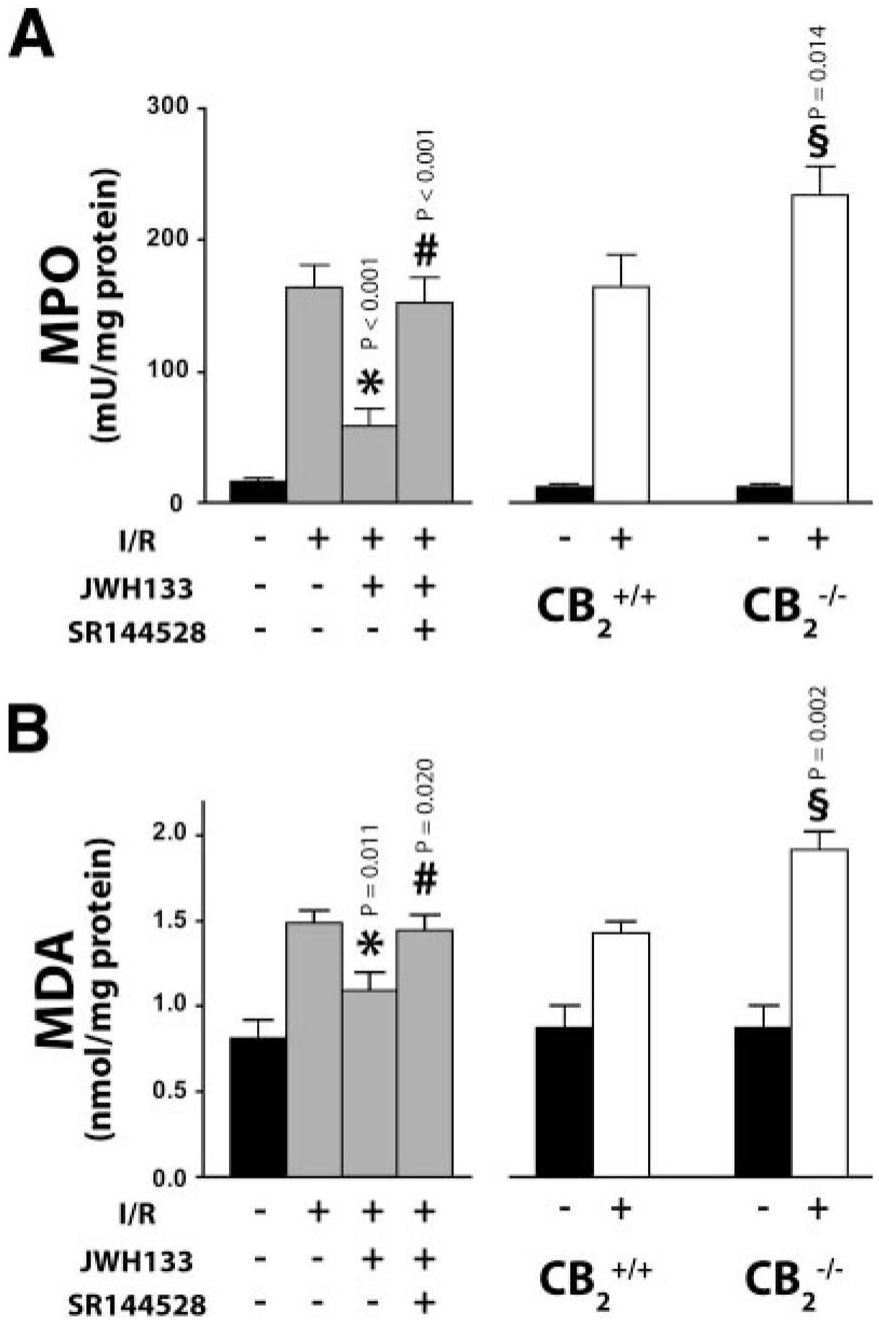

Figure 2.

Effect of CB_2 receptor modulation on neutrophil infiltration and lipid peroxidation in liver I/R. *A)* Liver myeloperoxidase (MPO) activity. Left: Sham (*n*=16) or 60/90 min I/R-exposed mice pretreated with vehicle (*n*=25), JWH133 (20 mg/kg, *n*=14) or SR144528 (3 mg/kg) in combination with JWH133 (*n*=8). Right: Sham $CB_2^{+/+}$ (*n*=8) and $CB_2^{-/-}$ (*n*=6) mice, or $CB_2^{+/+}$ (*n*=19) and $CB_2^{-/-}$ (*n*=21) mice exposed to 60/90 min I/R. *B)* Liver malonyldialdehyde (MDA) level. Left: Sham (*n*=10) or 60/90 min I/R-exposed mice pretreated with vehicle (*n*=18), JWH133 (20 mg/kg, *n*=6), or SR144528 (3 mg/kg) in combination with JWH133 (*n*=6). Right: Sham $CB_2^{+/+}$ (*n*=6) and $CB_2^{-/-}$ (*n*=8) mice, or $CB_2^{+/+}$ (*n*=9) and $CB_2^{-/-}$ (*n*=10)

mice exposed to 60/90 min I/R. (*P<0.05: I/R in vehicle- *vs*. JWH133-treated; #P<0.05: I/R in JWH133-*vs*. SR144528+JWH133- treated; §P<0.05: IR in $CB_2^{-/-}$*vs*. $CB_2^{+/+}$).

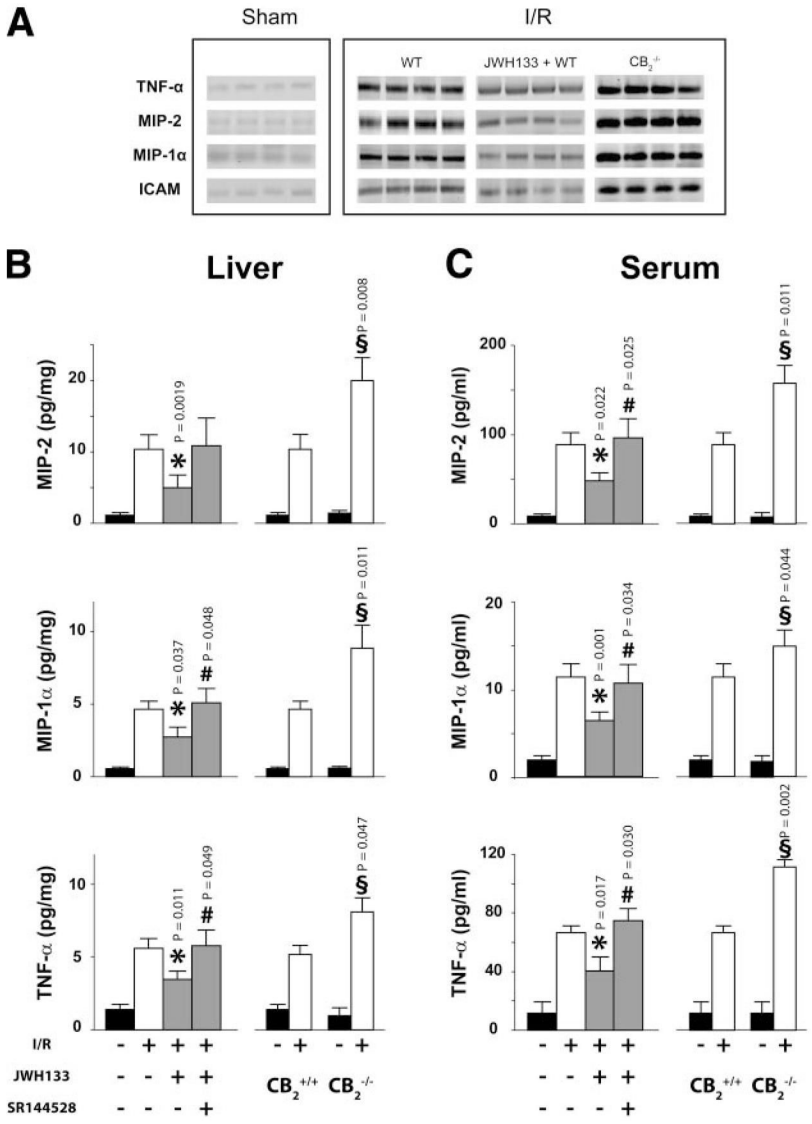

Figure 3.

CB_2 receptor agonist decreases proinflammatory markers in serum and liver. *A)* TNF-α, MIP-2, MIP-1α, and ICAM-1 expression detected by RT-PCR (*n*=4). *B, C)* MIP-2, MIP-1α, and TNF-α levels in liver tissue and serum, measured by ELISA. Left: Sham (*n*=10) or 60/90 min I/R-exposed mice pretreated with vehicle (*n*=12), JWH133 (20 mg/kg, *n*=8), or SR144528 (3 mg/kg) in combination with JWH133 (*n*=10). Right: Sham $CB_2^{+/+}$ (*n*=6) and $CB_2^{-/-}$ (*n*=5) mice or $CB_2^{+/+}$ (*n*=11) and $CB_2^{-/-}$ (*n*=13) mice exposed to 60/90 min I/R. (**P*<0.05: I/R in vehicle- *vs*. JWH133-treated; #*P*<0.05: I/R in JWH133- *vs*. SR144528+JWH133-treated; §*P*<0.05: IR in $CB_2^{-/-}$ *vs.* $CB_2^{+/+}$).

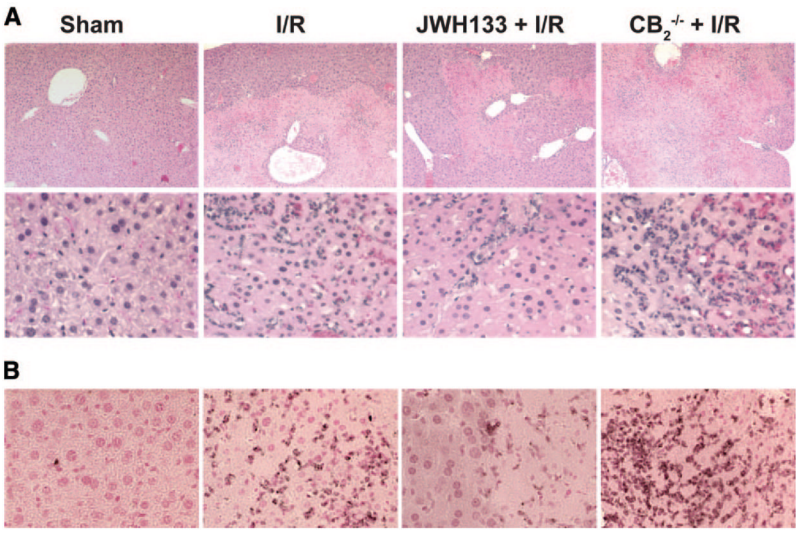

Figure 4.

CB_2 receptor agonist decreases histological damage and neutrophil infiltration 24 h following ischemia. Representative liver sections of sham mice, of mice exposed to 1 h/24 h I/R with vehicle or JWH133 pretreatment and of $CB_2^{-/-}$ mice exposed to 1 h/24 h I/R. *A)* Hematoxylin and eosin staining. *B)* Myeloperoxidase staining (brown) contrastained with nuclear fast red. Similar histological profile was seen in 3–4 livers/group.

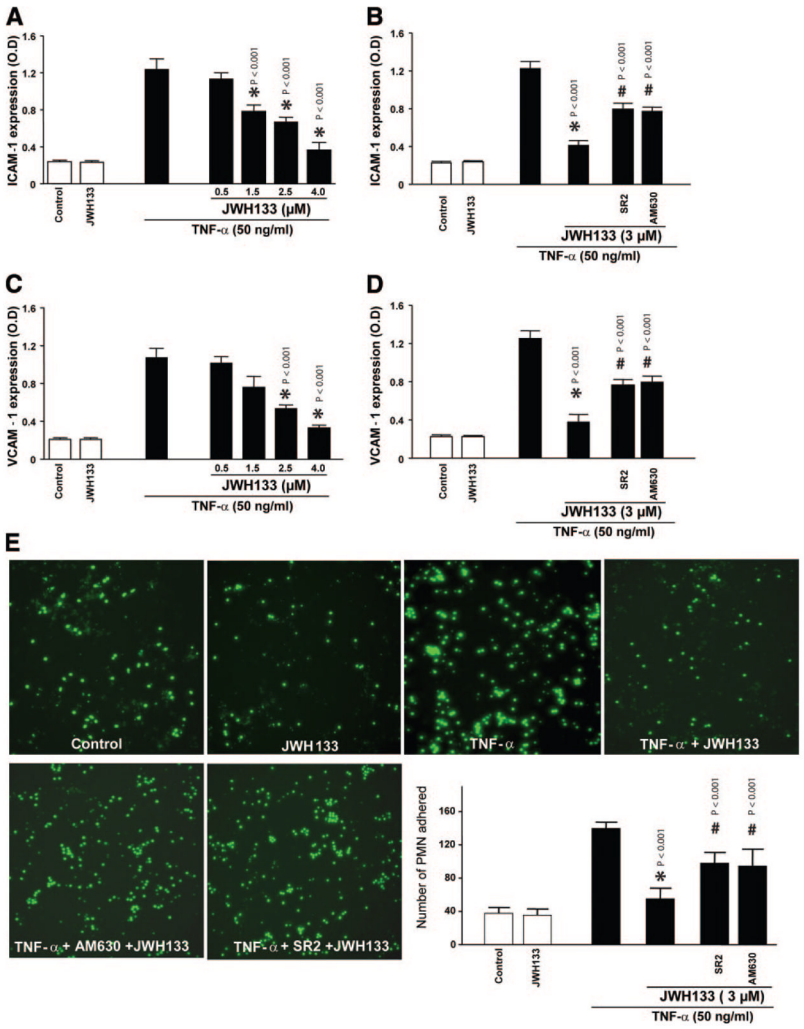

Figure 5.

CB_2 receptor agonist decreases TNF-α-induced overexpression of ICAM-1 and VCAM-1 in human liver sinusoidal endothelial cells. *A, B)* ICAM-1 expression; (*C, D*) VCAM-1 expression. *E)* TNF-α-induced neutrophil adhesion to human liver sinusoidal endothelial cells. Representative images and quantification of human neutrophil adhesion to human liver endothelial cells. (**P*<0.05: TNF-α *vs*. TNF-α+JWH133-treated; #*P*<0.05: TNF-α+JWH133-treated *vs*. TNF-α+JWH133+SR2 -or AM630-treated).

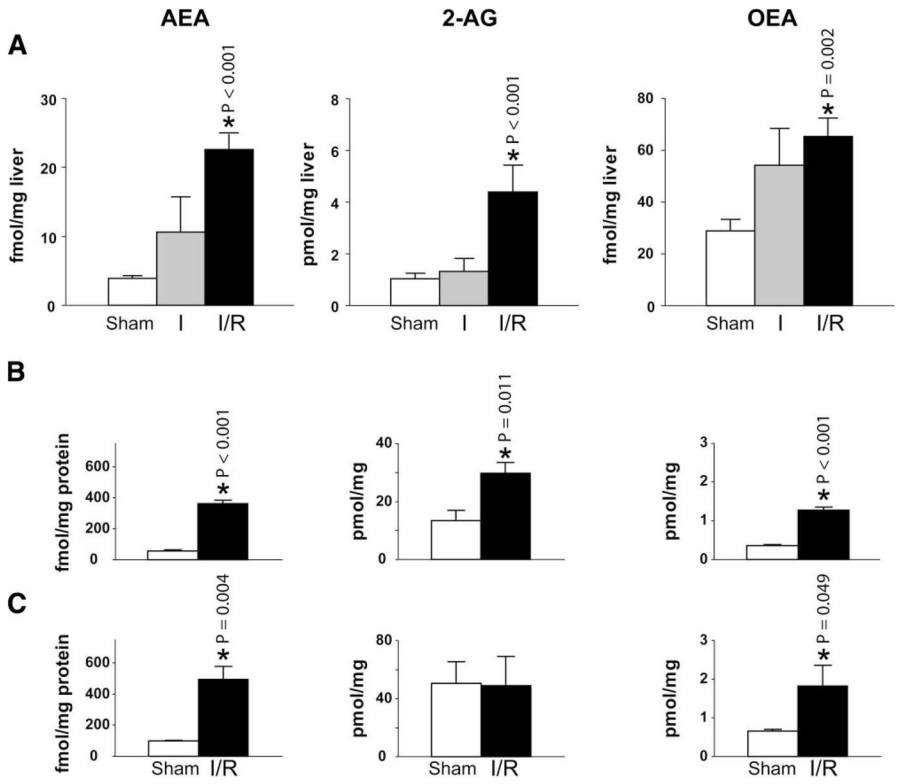

Figure 6.

I/R increases hepatic endocannabinoid levels. *A*) Endocannabinoid (anandamide [AEA], 2-arachidonoylglycerol [2-AG] and oleoylethanolamide [OEA]) levels in liver tissue in sham mice (*n*=19) and in mice exposed to 60 min ischemia (I; *n*=5) or 60/90 min I/R (I/R; *n*=13). *B*) Endocannabinoid levels in hepatocytes isolated from sham (*n*=8) or 60/90 min I/R-exposed mice (*n*=6). Each experiment represents a pool of 2 animals. *C*) Endocannabinoid levels in Kupffer cell/endothelial cell fraction isolated from sham (*n*=4) or I/R-exposed mice (*n*=5). Each experiment represents a pool of 6–8 animals. (**P*<0.05 sham *vs*. I/R).

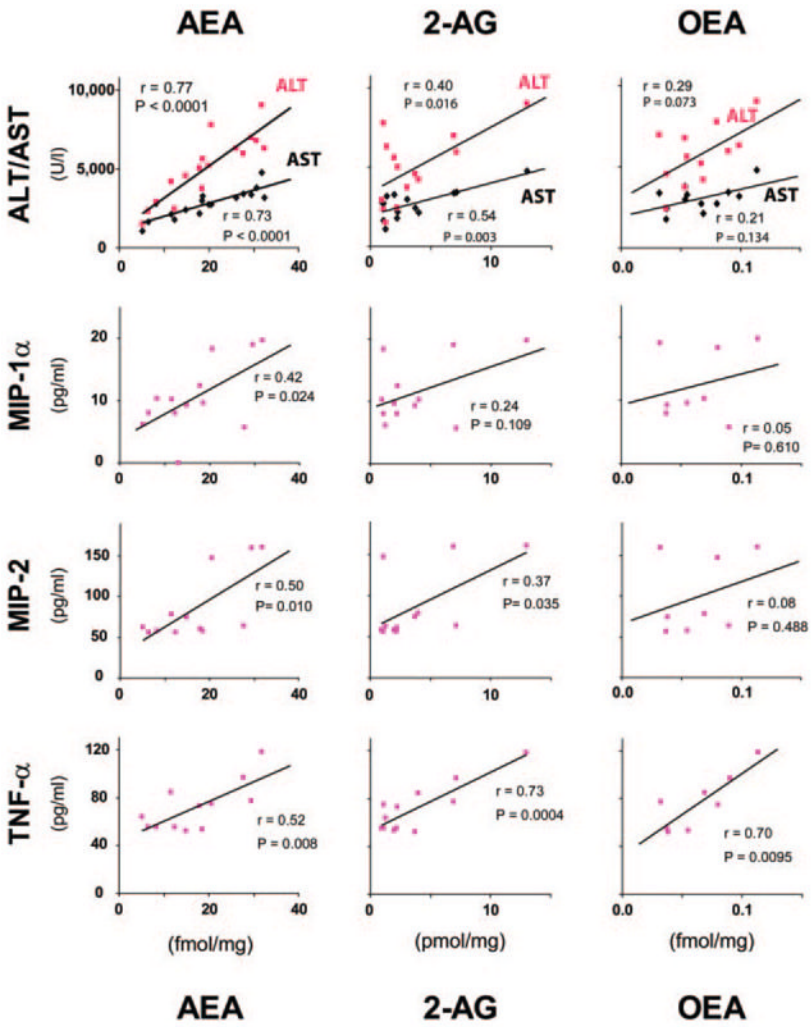

Figure 7.

Endocannabinoid levels positively correlate with markers of tissue damage and inflammation. Correlation between tissue endocannabinoid (AEA, 2-AG, and OEA) levels and serum transaminases (AST, ALT), serum MIP-1α, MIP-2, and TNF-α levels in mice exposed to 60/90 min I/R. Pearson coefficients (r) and *P*-values were calculated for each comparison.

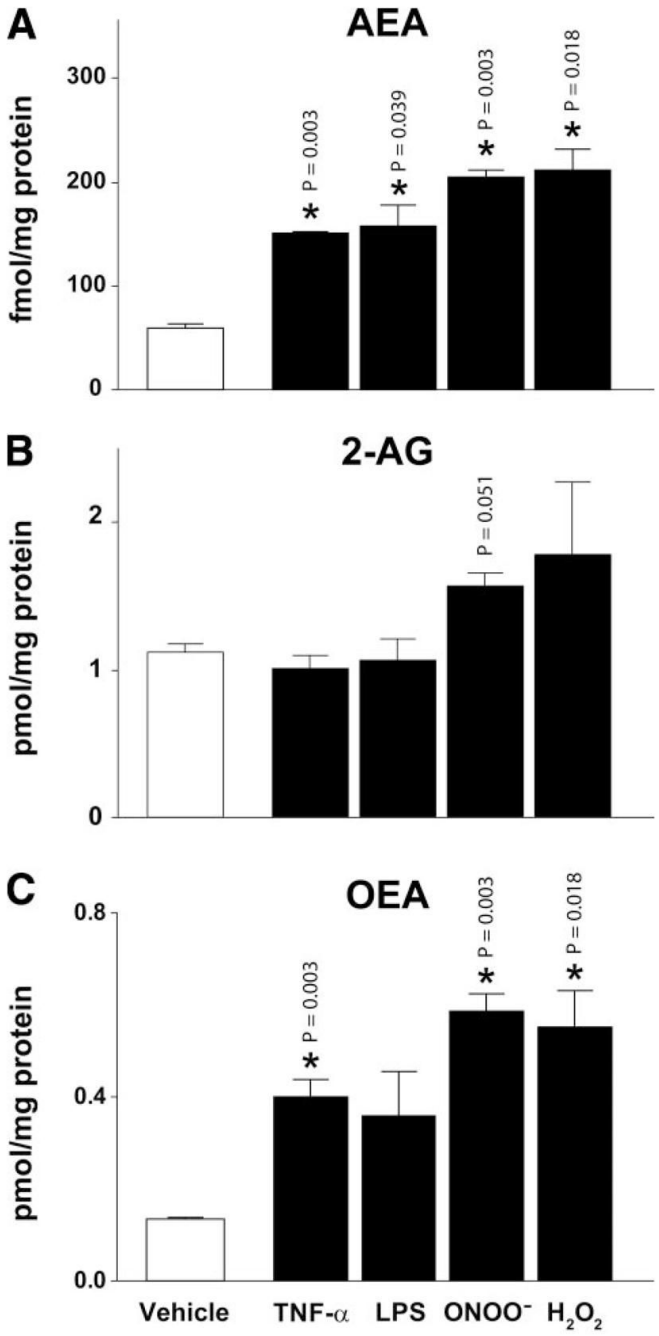

Figure 8.

Inflammatory stimuli and oxidants increase endocannabinoids in primary hepatocytes *in vitro*. Endocannabinoid (*A*, anandamide [AEA], *B*, 2-arachidonoylglycerol [2-AG] and *C*, oleoylethanolamide [OEA]) levels in primary hepatocytes in vehicle or treated with TNF-α, LPS, peroxynitrite ($ONOO^-$) and H_2O_2 (*P<0.05 vehicle *vs*. treatment).

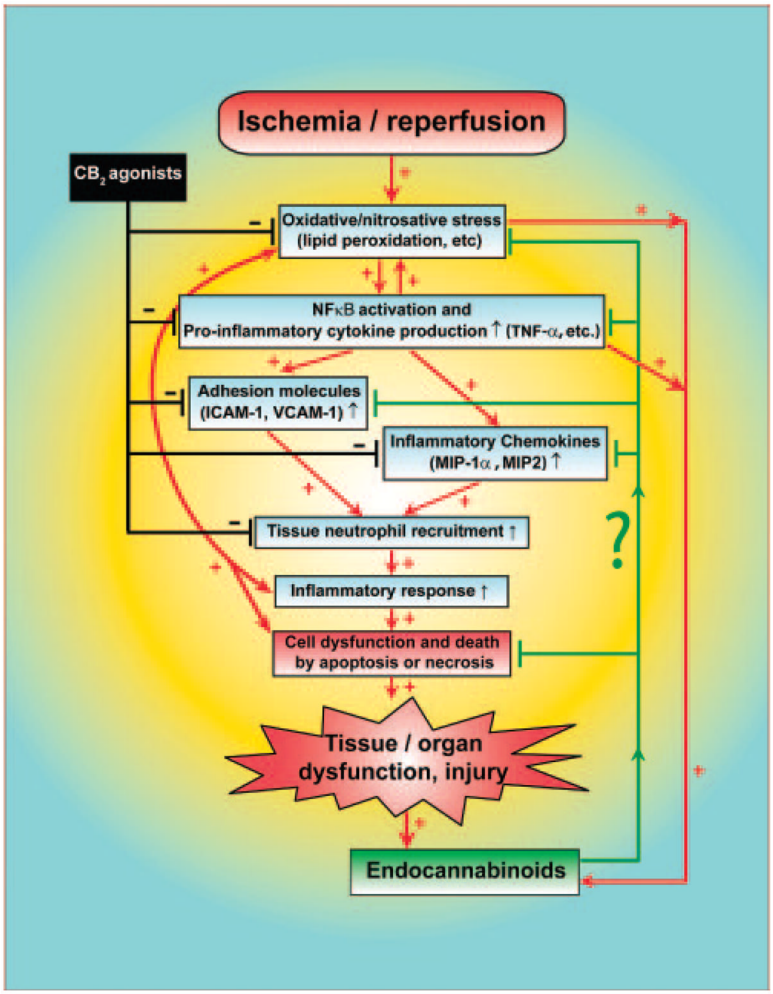

Figure 9.
Schematic diagram of the proposed role of endocannabinoids and CB_2 receptor activation in ischemia/reperfusion injury. Lines or arrows indicate inhibition (black), activation (red) or modulation (green).

TABLE 1

Effect of intraperitoneally injected 20 mg/kg JHW133 on hemodynamic parameters in C57BL6 mice

	Baseline	10 min	30 min	60 min
MAP (mmHg)	82.7 ± 0.2	85.6 ± 3.7	80.5 ± 1.3	82.7 ± 1.9
LVSP (mmHg)	105.8 ± 1.6	106.3 ± 3.5	100.8 ± 2.2	103.4 ± 2.7
HR (beat/min)	468.3 ± 9.5	469.0 ± 13.6	433.6 ± 27.6	447.5 ± 22.3
+dP/d*t* (mmHg/s)	9607.1 ± 553	10184.2 ± 1130.6	9354.2 ± 1608.6	9887.5 ± 1230.9
−dP/d*t* (mmHg/s)	7099.0 ± 660.6	6791.7 ± 859.9	6778.3 ± 1051.0	7052.5 ± 1316.8
CO (ml/min)	11.8 ± 0.2	12.1 ± 0.2	11.4 ± 0.6	11.6 ± 0.6
TPR (mmHg·ml^{-1}·min)	7.0 ± 0.1	7.1 ± 0.2	7.1 ± 0.4	7.2 ± 0.5

MAP, mean arterial pressure; LVSP, maximal left ventricular systolic pressure; HR, heart rate; +dP/dt, systolic left ventricular pressure increment; −dP/d*t*, diastolic pressure decrement; CO, cardiac output; TPR, total peripheral resistance. Values are mean ± SEM of 4 experiments in each group.

TABLE 2

Baseline hemodynamic parameters in $CB_2^{-/-}$ and $CB_2^{+/+}$ mice measured by Millar pressure-volume conductance catheter system

	$CB_2^{+/+}$	$CB_2^{-/-}$	P^1
HR (beat/min)	473.1 ± 14.4	475.3 ± 10.5	0.50
MAP (mmHg)	89.1 ± 3.5	86.4 ± 2.0	0.69
LVESP (mmHg)	102.4 ± 4.0	98.9 ± 1.8	0.68
LVEDP (mmHg)	4.0 ± 1.4	2.8 ± 0.7	0.52
CO (ml/min)	13.1 ± 0.5	12.6 ± 0.6	0.64
Stroke volume (μl)	27.7 ± 0.4	26.7 ± 0.6	0.51
EF (%)	59.6 ± 3.6	59.4 ± 2.4	0.53
SW (mmHg. μl)	2426.0 ± 65.9	2267.0 ± 144.7	0.68
+dP/d*t* (mmHg/s)	8819.9 ± 661.9	9065.2 ± 377.0	0.28
−dP/d*t* (mmHg/s)	6796.1 ± 322.4	7095.9 ± 376.0	0.27
τ (Weiss; ms)	7.2 ± 0.4	6.6 ± 0.2	0.22
τ (Glantz; ms)	11.4 ± 0.6	10.5 ± 0.1	0.13
TPR mmHg·ml^{-1}·min	6.9 ± 0.4	7.0 ± 0.4	0.73

Values are mean ± SEM of 7 to 8 experiments. HR, heart rate; MAP, mean arterial pressure; LVESP, left ventricular end-systolic pressure; LVEDP, left ventricular end-diastolic pressure; CO, cardiac output; EF, ejection fraction; SW, stroke work; +dP/d*t*, systolic pressure increment; −dP/d*t*, diastolic pressure decrement; **τ**, relaxation time constant; TPR, total peripheral resistance.